



EFFECT OF TRANSITION METAL ION SUBSTITUTION ON MAGNETIC STRUCTURE AND PROPERTIES OF La-Sr HEXAFERRITES AT NANOSCALE

PAWADE S.A.^{1*}, REWATKAR K.G.² AND NANOTI V.M.³

¹Department of Applied Physics, Rajiv Gandhi College of Engineering research & Technology, Chandrapur, MS, India.

²Department of Physics, Dr. Ambedkar College, Dikshabhumi, Nagpur, MS, India.

³Department of Applied Physics, Priyadarshini College of Engineering, Nagpur, MS, India.

*Corresponding Author: Email- asheela05@gmail.com

Received: February 28, 2012; Accepted: March 06, 2012

Abstract- Al-substituted M-type hexaferrite is a highly anisotropic ferromagnetic material. In the present study, microwave assisted Solgel auto-combustion route using urea as a reductant and nitrates as oxidants of synthesis for $\text{SrLa}_y\text{Al}_x\text{Fe}_{12-x-y}\text{O}_{19}$ ($y=1; 0 \leq x \leq 8$) powders were explored and their microstructure, grain morphology, magnetic properties, examined. X-ray diffraction (XRD), transmission electron microscopy (TEM), a vibrating sample magnetometer (VSM), were used to characterize the powders. The TEM analysis revealed that a powder with a smaller particle size, near single-domain structure, uniform grain morphology, and smaller shape anisotropy. The synthesis technique also significantly affected the magnetic properties. The grain size was found to be a key factor affecting the property of the powder. (XRD) studies reveal that microwave-assisted combustion synthesis route yields materials with higher degree of compositional stability and phase purity. Both a and c lattice parameters calculated and found to decrease with increasing Al content. The effects of Al³⁺ ions on the Strontium Lanthanum ferrites were reported and discussed in detail. The site preference of Al³⁺ and magnetic properties of the ferrites have been studied using hysteresis. The results show that the magnetic properties are closely related to the distributions of Al³⁺ ions on the five crystallographic sites. The saturation magnetization slowly decreases, however, the coercivity decreases with Al concentration. The magnetization results indicate that the Al³⁺ ions preferentially occupy the 2a, 12k, and 4f₂ sites. This confirms the use of samples in the various applications of digital data devices. Further attempts could lead to investigate their use in data storage devices, such applications favor nano-sized magnetic materials.

Keywords- Strontium ferrite, X-ray density, porosity, magnetization, coercivity, retentivity

Citation: Pawade S.A., Rewatkar K.G. and Nanoti V.M. (2012) Effect of Transition Metal Ion Substitution on Magnetic Structure and Properties of La-Sr Hexaferrites at Nanoscale. International Journal of Knowledge Engineering, ISSN: 0976-5816 & E-ISSN: 0976-5824, Volume 3, Issue 1, pp.-31-35.

Copyright: Copyright©2012 Pawade S.A., et al. This is an open-access article distributed under the terms of the Creative Commons Attribution License, which permits unrestricted use, distribution, and reproduction in any medium, provided the original author and source are credited.

Introduction

The hexagonal M-type hard hexaferrites have attracted much attention as the most widely used permanent magnets, which account for about 90% of the annual production of permanent magnets. These ferrites are perspective materials for developing such permanent magnets and high density perpendicular recording media, due to their high uniaxial magneto-crystalline anisotropy and chemical stability [1] with proper doping. The properties of this ferrite are largely dependent on the processing routes used for its fabrication [2-3].

Due to perfect chemical stability, good thermal durability, carrier resistivity, unique electrical and magnetic properties, Strontium

hexaferrites have extensive applications in recording devices [4], telecommunication [5] magneto-optical and microwave devices [6]. These materials cover a wide field of technological applications from microwave to radio frequencies due to its high electrical resistivity.

The properties of ferrites are strongly influenced by composition and synthesis method.

The rare earth substitution was employed to inhibit the grains growth [7] and to promote ferritization reaction [8]. The lanthanides also improve the mechanical materials hardness [9]. The experiments carried out by Dung [10] showed that the La substitutions improve hard magnetic properties of Sr hexaferrites.

In the present investigation we have synthesized M type nano sized Al^{+3} doped Sr hexaferrites by applying microwave assisted Sol-gel auto combustion process and we systematically amount on properties Viz crystal structure, saturation magnetization (M_s), Coercivity (H_c) and retentivity (M_r).

Experiment

The large number of preprational techniques have been reported earlier. Viz. solid state method, aerosol pyrolysis, co-precipitation method, hydrothermal method, salt method, micro emulsion method. These conventional methods require repeated grinding and calcination which invariably contaminate the powders.

The better method popularly known as microwave assisted 'Sol-gel Auto combustion' is employed to synthesize substituted magnetoplumbites by virtue of many advantages of this technique like facile operation, low anneal or calcination temperature, energy efficient and a short reaction rate, etc. In microwave oven heat is generated within the sample volume itself by the interaction of microwaves within the sample volume by the interaction of microwaves with the material on molecular level which leads uniform heating. In addition, the sol-gel combustion route gives ultra fine powder of nano particles with better particle size distribution, excellent chemical homogeneity and more probability of formation of single domain structure [11].



Fig. 1- Experimental set up (peak reaction)

M-type Al^{+3} substituted Sr hexaferrites were synthesized by sol-gel combustion method. All chemicals used for this synthesis were of analytical reagent grade. Stichometric amount of metal nitrates. Viz $\text{Sr}(\text{NO}_3)_2$, $\text{La}(\text{NO}_3)_3 \cdot 6\text{H}_2\text{O}$, $\text{Fe}(\text{NO}_3)_3 \cdot 6\text{H}_2\text{O}$ $\text{Al}(\text{NO}_3)_3 \cdot 9\text{H}_2\text{O}$, viz. were dissolved in triple filtered deionised water. Urea $[(\text{NH}_2)_2\text{CO}]$ was also dissolved in deionised water and is used as reducing agent to supply requisite energy to initiate exothermic reaction amongst oxidants. All solutions as prepared were mixed together to form a homogeneous yellow brown transparent aqueous solutions, and also treated by ultrasonic vibrator for half an hour. After that, mixed solution was kept in room temperature for 2 hrs. The yellow brown transparent solution was heated in microwave oven so that it gets concentrated slowly without producing any precipitation but change its viscosity and color until it turns into brown gel. After about 10-15 minutes of irradiation the gel swelled into foam and underwent self propagating combustion reaction changing brown gel into fluffy mass which is further ground into black powder. The resulting black ashes were grounded in an agate pestle and mortar put into alumina crucibles and then calcined at 800°C for 1 hr.

Calcined powders were ground and after adding polyvinyl alcohol, binder mixtures were shaped into pallets using hydraulic press under uniaxial pressure of 75 kNm^{-2} . These pallets of each composition were then sintered at 1200°C in electric furnace for 7-8 hours. During sintering process crystallization gave rise to a hexagonal polycrystalline phase.

The phase identification of the gel precursor, the as-burnt and calcined powders was performed using X-ray diffraction (XRD) on a PW-1710 Philips Holland X-ray diffractometer using Cu K α radiation ($\lambda=1.5405\text{\AA}$). The average crystallite size of the powders was measured by X-ray line-broadening technique employing the Scherrer formula. The particle morphology was examined by a transmission electron microscope (TEM). Magnetic properties were measured by a vibrating sample magnetometer (VSM) with a maximum applied field of 15 KOe. While the magnetic susceptibility measurements were carried out on Gouy's balance in the temperature range 300 -700 K.

Result and discussion

The X-ray pattern showed a single crystalline phase without any trace of impurity indexed as hexagonal magneto plumbite structure [12]. By isomorphism of the M compounds the space group is presumed to be D_{6h}^{19} or $P6_3/mmc$ [13] as shown in figure 1. Reported values of bulk Sr-M hexaferrites are $a=5.88\text{\AA}$ and $c=23.03\text{\AA}$. [14]

As shown in the table 1, the lattice parameter 'a' and 'c' shows slight variation with substitution of Al^{+3} ions in reference to Table 1 This is in agreement with the fact that all hexagonal ferrite exhibits constant lattice parameter 'a' variable 'c'

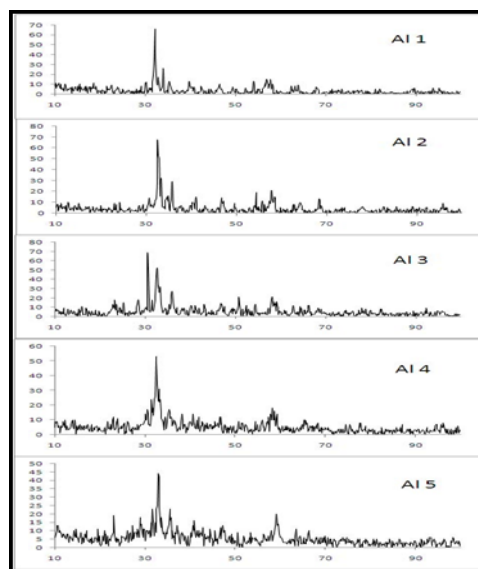


Fig. 2- XRD patterns for $\text{SrLaAl}_x\text{Fe}_{11-x}\text{O}_{19}$

It also indicates that change of easy magnetized c-axis is larger than a-axis with Al^{3+} ions substitution [15]. A variation in the values of the lattice parameter is observed because of the fact that atomic radii of Al^{+3} (0.53\AA) is smaller than Fe^{+3} (0.67\AA). The decrease in cell parameter agrees well with the result in BaM system [16-18]. The replacement of Fe^{+3} by Al^{+3} ions have been investigated as resemblance of ionic radii of former with substituent fairly matches. It is further noted that the former ions were very easily re-

placed at substitution ratio $0 \leq x \leq 8$ without changing crystal symmetry. The radii of Al^{+3} , Cr^{+3} and Fe^{+3} are 0.53 Å, 0.64 Å and 0.67 Å respectively. The Al^{+3} is easier than Cr^{+3} to substitute for Fe^{+3} to enter the lattice of strontium ferrite.

The Transmission Electron Micrographs (TEM) gave in Fig. 2(a)-(d) reveal the remarkable changes in the microstructure, grain size, porosity and homogenous particle size distribution. Therefore it could be attributed that these remarkable changes are observed as a perturbation of many dependant parameters like time of synthesis, temperature, process of annealing, intermittent quenching, grinding, etc. [19-20]. It is also come to the notice that the presence of the large crystalline agglomerations is composed of very small discrete crystallites in the samples at the temperature of synthesis. The particle size is determined with the help of TEM studies [21]. The size is found to be on an average 50nm confirming the nanoparticle size of the hexaferrites.

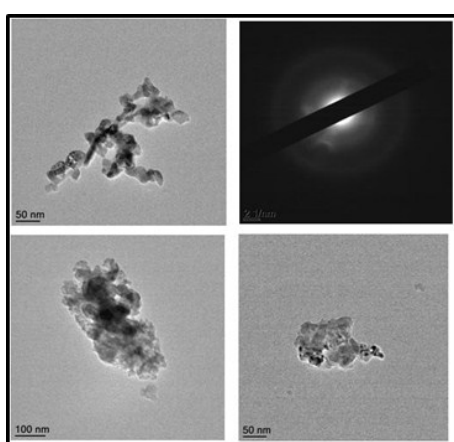


Fig. 3- TEM results for sample $SrLaAl_xFe_{11-x}O_{19}$

The crystal structure of magnetoplumbite M-type components (SG: $P6_3/mmc$) can be described as superimposition of two structural blocks, namely the R-block with composition $(SrFe_6O_{11})^{2-}$ and the S-block with composition $(Fe_6O_8)^{2+}$. The metallic cations are distributed within five different crystallographic sites with octahedral and tetrahedral environment in table 2 (Gorter spin colinier model), we have summarized the crystallographic characteristics of the five different sublattices together with the spin alignments corresponding to the collinear magnetic structure proposed by [22].

Table 2- Crystallographic sites of Fe ion

Sub lattice	Co-ordination	Number of ions	Spins
12K	Octahedral	6	Up
4f ₁	Tetrahedral	2	Down
4f ₂	Octahedral	2	Down
2a	Octahedral	1	Up
2b	Trigonal bi- pyramidal	1	Up

For hexaferrites testing magnetic properties is of great importance. The stoichiometry of the samples is so chosen that desired improvement in coercivity, remanance magnetization, saturation magnetization can be expected. (23,24) The coercivity and remanance magnetization of the synthesized samples is found to be from (5000---375 Oe) and (13.1370-0.1491 emu/gm.) respectively so that they can be used in the application described earlier. The Curie temperature of the samples is found to be between (478-578) The tem-

perature is found to be increasing with the increase in composition of transition metal ion. (Al^{+3}) from (2 to 8). As observed from table 3.

The increase in the Curie temperature (T_c) indicates that some intersublattice exchange interaction are strongly diminished. The increase in Curie temperature may be attributed to the presence of nonmagnetic ions in the tetrahedral and octahedral sites. It has already been reported Obradors et.al. [25] that Al^{3+} ions occupy 2a, 12k and 4f₂ sites. Hysteresis loops in Figure 4 indicates that all the samples exhibit steep rise in magnetization at low applied field followed by a slow variation at high field. The large slope of hysteresis curve of undoped sample i.e. $x = 0$ at high field indicates unsaturated state and this slope falls with substitution of Al^{+3} ions. The reduction in anisotropy field, discussed later, is responsible for this variation.

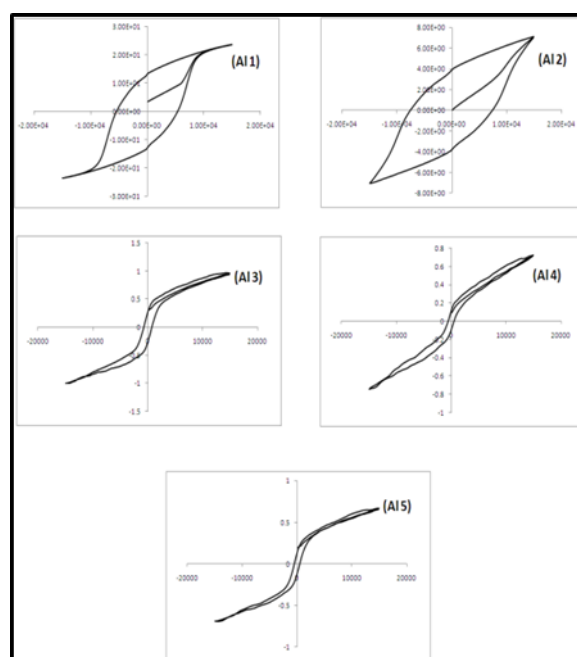


Fig. 4- Hysteresis Loop for $SrLaAl_xFe_{11-x}O_{19}$

Figure 4 shows the variation of all the above mentioned magnetic properties with annealing temperature for the pure strontium hexaferrite nanoparticles. The Saturation magnetization (M_s), Remanence (M_r) and Coercivity (H_c) decreases in room temperature and maximum value for each property is obtained at room temperature of 300 K. This behavior can be explained on the basis that the particle size which was explained by Alamholhoda [26]. It is also well known that particle size has a significant effect on the magnetic properties of materials. The particles smaller than the critical single domain size are mainly in single domain. On the other hand, the particle size becomes bigger than the critical value most of the particles exist in multi-domain.

Al^{+3} ions occupy 2a, 12k and 4f₂ sites, when the sites 2a, 2b, 12k and 4f₂ are occupied by non-magnetic ions the exchange interactions like 2a-12k, 2a-4f₁ and 4f₁-12k decreases. Out of this 4f₁-12k interaction is the strongest and has predominant influence on the magnetic parameters Albanese [27].

The basic magnetic properties originate from Fe^{+3} ions on both tetrahedral sites and octahedral sites. When Al^{+3} ions are substi-

tuted the Fe^{+3} ions decrease from Fe_{12}^{+3} to Fe_{12-x}^{+3} . This reduces the 2a-4f₁ and 4f₁-12k exchange interaction and hence the magnetization.

It has been observed from the Table 2 that as the concentration of the doping element Al^{+3} increases the M_s and M_r decreases. This is because of agglomeration of particles or wide particle distribution which changes the magnetic properties of the particles. There is change from single domain to multi domain structure as reported by Huang [28].

H_c is decreasing as grain size is increasing. To explain the dependence of H_c on grain size by Relescu [29] proposed that the coercivity is due to pinning of the magnetization at the grain boundaries. Since surface to volume ratio decreases as the grain size increases smaller grains will have more boundaries to pin in the magnetization. We can say that Al^{+3} substitution causes the change of easy axis of magnetization from 'c' axis to basal plane. This fall of coercivity causes the change from hard ferrites to soft ferrites.

The reduction in saturation magnetization occurs due to low magnetic moment of Al^{+3} ions. The magnetic moments of Al^{+3} ions are not able to cancel out with spin down moments of Fe^{+3} ions, thereby decreasing M_s . The magnetization are closely related to distribution of Al^{+3} ions on each crystallographic sites and then magnetic dilution or non collinear structure (spin canting) with the substitution of Fe^{3+} ions by lower magnetic moment ions.

It is known for Sr-M ferrites that the magnetic moment of Fe^{+3} ions arranged collinearly due to existence of super exchange interaction that is to say that it is the superexchange interaction to determine the orientation of magnetic moments of Fe^{+3} ions. When Fe^{+3} is replaced by other divalent or trivalent or tetravalent combination the change in magnetic characters i.e. magnetic intensity occurs, this is called canting of spin structure. In addition to this the substitution causes decrease of Bohr magneton according to M-type structure by Lotgering [30].

Conclusion

The X-ray diffraction studies confirm the formation of hexaferrites and the a and c values of the sample supports this confirmation. Structural studies have confirmed the space group of samples to be p63/mmc. From TEM of the sample, average particle size is found to be in nanorange (≈ 50 nm). The reduction of particle size of hexaferrites to nanorange helps to improve many magnetic properties mentioned earlier. The hysteresis curve of the sample at different concentration attributes that such sample specially synthesized by microwave induced sol-gel combustion route can hold the data confirming their use in storage devices [31]. The magnetic characters of the samples are observed to be of immense vital improvisation. It is known that the nanohexa ferrites with such special magnetic properties are highly useful in Data storage applications [32,33].

References

- [1] Relescu N., Doroftei C., Relescu E. and Popa P.D. (2008) *Journal of Alloys and Compounds*, 451 492-49
- [2] T. Fujiwara (1985) *IEEE Tran. Magn.* 21,, 1480-1484.
- [3] Speliotis D. E. (1995) *IEEE Tran. Magn.* 31, 2877-2881.
- [4] Rewatkar K.G., Prakash G.S. and Kulkarni D.K. (1996) *Mater. Lett.* 28, 365-368.
- [5] Palla B.J., Shah D.O., Casillas P.G. and Aquino J.M. (1999) *J. Nanopart. Res.*, 1, 215.
- [6] Costa A.C.F.M., Tortella E., Morelli M.R. and Kininami R.H.G.A. (2003) *J. Magn. Magn. Mater.*, 256, 174.
- [7] Qiu J., Gu M. and Shen H. (2005) *J. Magn. Magn. Mater.* 295, 263,
- [8] Taguchi H. (1997) *J. Phys. IV France* 7, C1-299..
- [9] Troczynski T.B. and Nicholson P.S. (1989) *J. Am. Ceram. Soc.* 72, 1488.
- [10]Dung N.K., Minh D.I., Cong B.T., Chau N. and Phue N.X. (1997) *J. Phys. IV France*, C1-313.
- [11]Lisjak D. and Drofenik M. (2004) *Journal of the European Ceramic Society* 24 1845.
- [12]Sharrock M. (1989) *IEEE Trans. Magn. MAG.* 25, 4374.
- [13]Sable S.N., Rewatkar K.G. and Nanoti V.M. (2009) *Mater. Sci. Eng.*, B168,156
- [14]Livingston D. (1981) *J. Appl. Phys.* 522-541.
- [15]Giriya M.N. (2008) *Ph.D. Thesis, Study of Synthesis, Thermo-Electric and Magnetic Properties of M-Type Q uaternary Ion Doped Mixed Ferrites.*
- [16]Haneda K. and Kojima H. (1973) *Japan J. Appl. Phys.* 12, 355.
- [17]Darokar S.S., Rewatkar K.G. and Kulkarni D.K. (1998) *Materials Chemistry and Physics* 56,84-86
- [18]Rodriguez J., Tejada J. and Joubert J.C. (1984) *IEEE Trans. Magn.*, 20 1636
- [19]Sibiu and Romania (2007) *The 5th International on New Research Trends in Materials Science.*
- [20]Thompson S., Shirlcliffe N.J., O'Keefe E.S., Appleton S. and Perry C.C. (2005) *J. Magn. & Magn. Materials*, 292,100-10.
- [21]Rewatkar K.G., Patil N.M. and Gawali S.R. (2005) *Bulletin of materials Science* 28(6), 585-587.
- [22]Relescu N., Doroftei C., Relescu E. and Popa P.D. (2008) *Journal of Alloys and Compounds*, 451, 492-496.
- [23]Hessien M.M., Rashad M.M. and El-Barawy K. (2008) *J. Magn. and Magn. Materials* 320, 336-343.
- [24]Litsardakis G., Manolakis I., Serletis C. and Efthimiadis K.G. (2007) *J. Magn. and Materials* 316, 170-17
- [25]Obradors X., Isalgne A.E., Collomb A., Lamb A., Pemet a, M., Pereda J.A., Tejada J. and Joubert J.C. (1986) *J. Phys. C.*
- [26]Alamolhoda S., Ebrahimi S.A.S. and Badiei A. (2006) *J. Magn. Mater.*, 303, 69.
- [27]Albanese G., Carbucicchio M. and Deriu A. (1978) *Phy. Stat. Solid, (A)* 23, 351.
- [28]Huang J., Ding F. and Kun. (1987) *J. Technical Report. Jin-Chuan Radio & Appliance Factory.*
- [29]Relescu N. and Cuciureanu E. (1970) *Phys. Stat. Sol.* 3, 873.
- [30]Lotgering F., Vromans P. and Huyberts M. (1980) *J. App. Phys.*, 51, 5913.
- [31]Schaubert D. (2009) *The Antenna Applications Symposium*, 52, 24.
- [32]Rendale M.K., Kulkarni S.D. and Puri V. (2009) *Microelctronics International Journal*, 26, 43-46.
- [33]Patron L., Mindru I. and Marinescu G. (2009) *Dekker Encyclopedia of Nanoscience & Nanotechnology*, second edition.

Table 1- X-Ray Diffraction Calculations for the samples SrLaAl_xFe_{11-x}O₁₉

Sample	Fomuala	x	a (Å)	c(Å)	Bulk Density (B)	V gm/cm ³	X-ray density gm/cm ³	Porosity (P)	Particle Size (A ^o)
Al-1	Sr La Fe ₁₁ O ₁₉	0	5.8000	22.3626	2.6367	665.72	5.7105	53.82	8.0362
Al-2	Sr La Al ₂ Fe ₉ O ₁₉	2	5.9486	22.0848	2.5427	665.57	5.4235	53.12	49.2190
Al-3	Sr La Al ₄ Fe ₇ O ₁₉	4	5.8116	21.5120	2.2144	672.74	5.3819	49.87	18.0139
Al-4	Sr La Al ₆ Fe ₅ O ₁₉	6	5.8100	21.1660	2.1078	696.77	4.6347	48.21	7.2398
Al-5	Sr La Al ₈ Fe ₃ O ₁₉	8	5.7943	21.0875	2.0634	707.88	4.2942	46.12	10.3546

Table 3- VSM Calculations for SrLaAl_xFe_{11-x}O₁₉

Sr. No.	x	Molecular Formula	Ms (emu/g)	Mr (emu/g)	Hc (Oe)	(μ _B)	(K) Tc	Tc
1	0	Sr La Fe ₁₁ O ₁₉	23.535	13.137	5000	4.8231	0.0588	478
2	2	Sr La Al ₂ Fe ₉ O ₁₉	7	3.65	7130	1.3625	0.0250	488
3	4	Sr La Al ₄ Fe ₇ O ₁₉	0.9787	0.3479	750	0.1804	0.000367	517
4	6	Sr La Al ₆ Fe ₅ O ₁₉	0.712	0.1685	625	0.1239	0.000222	558
5	8	Sr La Al ₈ Fe ₃ O ₁₉	0.659	0.1491	375	0.1078	0.000164	578